Article

Magnetic Molecularly Imprinted Chitosan Combined with a Paper-Based Analytical Device for the Smartphone Discrimination of Tryptophan Enantiomers

Abdelhafid Karrat[1,2], Juan José García-Guzmán[1]; José María Palacios-Santander[1,*], Aziz Amine[2,*], Laura Cubillana-Aguilera[1]

[1] Institute of Research on Electron Microscopy and Materials (IMEYMAT), Department of Analytical Chemistry, Faculty of Sciences, Campus de ExcelenciaInternacional del Mar (CEIMAR), University of Cadiz, Campus Universitario de Puerto Real, Polígono del Río San Pedro S/N, 11510, Puerto Real, Cádiz, Spain

[2] Laboratory of Process Engineering & Environment, Faculty of Science and Technology, Hassan II University of Casablanca, B.P. 146. Mohammedia, Morocco

* Correspondence: azizamine@yahoo.fr (A. Amine) ; .palacios@uca.es (J.M. Palacios-Santander)

Abstract: Enantiomers separation plays a critical role in pharmaceutical development, ensuring therapeutic efficacy, safety, and patent protection. It enables the production of enantiopure drugs, and enhances our understanding of the properties of chiral compounds. In this study, a straightforward and effective chiral detection strategy was developed for distinguishing between tryptophan (TRP) enantiomers. The approach involved the preparation of a magnetic molecularly imprinted chitosan (MMIC) for the sample preparation, which was combined with a nitrocellulose membrane (paper-based analytical device, PAD) integrated with D-TRP covalently-grafted polymethacrylic acid (PAD_PMA_D-TRP). The discrimination between TRP enantiomers was achieved using AuNPs as a colorimetric probe. Indeed, the presence of D-TRP rapidly induced the aggregation of AuNPs due to its strong affinity to PAD-PMA_D-TRP, resulting in a noticeable color change of the AuNPs from red to purple. On the other hand, L-TRP did not induce any color change. The chiral analysis could be easily performed with the naked eye and/or a smartphone. The developed method exhibited a detection limit of 3.3 µM and it was successfully applied to detect TRP in serum samples, demonstrating good recovery rates. The proposed procedure is characterized by its simplicity, cost-effectiveness, rapidity, and ease of operation.

Keywords: Chitosan; magnetic molecularly imprinted polymer; enantiomers discrimination; tryptophan; smartphone; paper-based analytical device

1. Introduction

The majority of drugs, pharmaceuticals, and biologically active compounds are mixtures of chiral isomers, which have similar chemical and physical properties. However, in most cases, one isomer exhibits the desired biological and toxicological effects, while the other may be inactive or have different pharmacological effects[1,2]. For instance, the tragic incident in the early 1960s involving thalidomide revealed that only the (R)-enantiomer provided pain relief, while the (S)-enantiomer caused severe deformities in unborn children [3]. Another example is TRP, which has two enantiomers with distinct activities[4,5]. L-TRP is a vital component of proteins and a precursor to melatonin and serotonin, which aids in sleep and mental health improvement. On the other hand, D-TRP, a non-protein amino acid, does not participate in the metabolic pathways of living systems,

 doi:10.20944/preprints202306.1250.v1

but it is commonly used in the synthesis of immunosuppressant and peptide antibiotics[6–8]. The importance of chiral molecules in pharmaceutical and biologically active compounds production has led to a significant demand for effective separation techniques to purify chiral molecules from racemic mixtures. Molecular imprinting is a promising method for separation, as it relies on the spatial structure of the target molecules [9,10].

Molecularly imprinted polymers (MIPs) are cross-linked polymers formed through polymerization of a functional monomer (or co-monomers) in the presence of a template and a crosslinking agent [11,12]. Once the template is removed, recognition cavities are created within the polymer, which selectively recognize the target molecule in a mixture of compounds [13,14]. MIPs find wide applications for various analytes such as viruses, bacteria, emerging pollutants, pharmaceutical drugs, and pesticides [15–17]. MIPs are largely used for the sample preparation and extraction of target analytes from complex matrices by its combination with magnetic nanoparticles (MNPs) [18–20]. This combination offers several advantages. Firstly, it enables selective extraction of target analytes from complex samples. Secondly, the magnetic properties of MNPs allow an efficient and rapid extraction, as they can be easily manipulated and separated using a magnet. Additionally, MIPs provide a robust and reusable platform for selective extraction, as they can be regenerated and reused multiple times [21,22].

Chitosan, a polysaccharide derived from chitin, is particularly suitable for MIP development due to its non-toxic, biocompatible, bioactive, and biodegradable properties. Its abundance of amino and hydroxyl groups allows it to react with various cross-linking agents for the MIPs preparation [23–25]. In recent years, the use of gold nanoparticles (AuNPs) as optical labels has resulted in the development of numerous sensors and biosensors [26,27]. The simplicity of AuNPs synthesis and its intense red color, visible to the naked eye, make it a popular choice. However, research on colorimetric chiral discrimination using metal nanoparticles is limited, and a straightforward device for this purpose is yet to be developed. Consequently, constructing a reliable, user-friendly, sensitive, and high-throughput assay for determining the enantiomers of chiral substances still remains a challenge.

A PAD is a low-cost, portable, and disposable device that utilizes paper as the primary substrate for performing analytical tests. It integrates various components, such as sample application zones, and detection zones for performing chemical or biological assays. The concept behind PADs is to leverage the properties of paper, such as its capillary action and porous structure, to facilitate fluid flow and reaction processes. The design typically involves creating channels on the paper surface to direct the movement of liquid samples and reagents [28,29]. PADs can be used for a wide range of applications, including clinical diagnostics, environmental monitoring, food safety testing, and drug detection. They often require minimal or no instrumentation, making them particularly suitable for resource-limited settings and point-of-need testing [30].

In this work, a magnetic molecularly imprinted chitosan (MMIC) was developed for the TRP extraction and combined with a PAD for the discrimination between the TRP enantiomers. The proposed PAD is based on a nitrocellulose membrane modified with D-TRP-grafted polymethacrylic acid (PMA_D-TRP) successfully leading to good chiral separation using AuNPs as colorimetric probe. The developed procedure holds promise for applications in pharmaceutical analysis, offering a reliable and user-friendly approach for chiral analysis.

2. Materials and Methods

2.1. Material and apparatus

Chitosan, $FeCl_3 \cdot 6H_2O$, $FeCl_2 \cdot 4H_2O$ sulfuric acid (H_2SO_4), L-TRP, D-TRP, methacrylic acid, ethylene glycol dimethylacrylate (EGDMA), azobisisobutyronitrile (AIBN), dimethylsulfoxide (DMSO), copper(II) chloride ($CuCl_2$), acetic acid (AcH), polyphosphoric acid (H_3PO_4), and boric acid (H_3BO_3) were purchased from Sigma-Aldrich (Steinheim,Germany). Membrane filters Nitrocellulose 0.45 μm, diameter 47 mm was purchased from Sigma-Aldrich.

 doi:10.20944/preprints202306.1250.v1

Scanning/transmission electron microscopy (STEM) images were acquired using FEI Nova NANOSEM 450 equipment (Thermo Fisher Scientific, USA) (resolution = 1nm). Fourier transform infrared (FT-IR) spectra were collected using aIR Affinity-1S spectrophotometer(Shimadzu, Japan), in theAttenuated Total Reflectance(ATR) mode and in the range of 4000–500cm^{-1}. UV absorption spectra were measured by a double beam UV/vis spectrophotometer, model T80+from PG Instruments (Leicestershire, England). The pictures for TRP discrimination were taken with an android Smartphone (13 MP, camera). Nanopure water was prepared by a Wasser lab Ultramatic Plus (type I) system (Navarra, Spain) and used in all experiments.

2.2. Synthesis of magnetite nanoparticles

The synthesis of Fe_3O_4 nanoparticles was carried out using the method described in reference [31]. In brief, a three-necked flask was prepared under a N_2 atmosphere, and a solution containing 13.56 g of $FeCl_3{\cdot}6H_2O$ and 4.96 g of $FeCl_2{\cdot}4H_2O$ dissolved in 250 mL of distilled water was prepared. Subsequently, 20 mL of ammonium hydroxide was introduced into the flask, and the mixture was vigorously stirred for 40 minutes at 80 °C. The resulting Fe_3O_4 nanoparticles were then collected using an external magnet and washed with distilled water to eliminate any residual chemicals. The obtained precipitate was finally dried at 50 °C in a vacuum oven.

2.3. Molecularly imprinted chitosan synthesis

The preparation method of MMIC was as follows. Initially, 100.0 mg chitosan was dissolved in 10.0 mL of 1.0% (v/v) aqueous acetic acid solution. At the same time, 6.0 mg of the template molecule TRP was added into the chitosan solution followed by the addition of 100 mg of $Fe_3O_4$and stirred at room temperature for 4 h. Subsequently, 0.5 M of sulfuric acid was added to the solution and stirred for 2 h. After that, the TRP template molecules were removed by ethanol solvent. A magnetic non-imprinted chitosan (MNIC) was prepared following the same procedure excepting for the template addition.

2.4. Gold nanoparticles synthesis

Gold sononanoparticles were synthesized according to our previous study [32]. Initially, a cylindrical glass vessel was placed in a water bath containing1.25 mL of a 1.0 mM $HAuCl_4$ aqueous solution. To ensure consistent temperature, the sample vessel remained in the water bath at ambient temperature throughout the process, as the local heating from sonication affects the solution temperature. After 4 minutes of sonication, 250 µL of a 38.8 mM sodium citrate dihydrate aqueous solution was added to the vessel. This addition caused an immediate change in the solution color to grey. Continuous sonication led to a subsequent transformation of the solution color to dark red after 5.5 minutes, indicating the formation of the AuNPs colloid.

2.5. Synthesis of D-TRP-grafted polymethacrylic acid (PMA_D-TRP)

PMA_D-TRP was prepared according to the following procedure: 20 mg of D-TRP was introduced into a beaker containing 50 mL of DMSO, followed by the addition of 700 µL of MAA and 10 mL of EGDMA. Then, 10 mg of $CuCl_2$ was added to link covalently the monomer to D-TRP and 3.3 mg of AIBN to initiate the polymerization process. The blend was deaerated with nitrogen for 5min and the reaction was carried out at 60°C for 15min using a domestic microwave. The obtained material was washed and dried in oven at 60 °C.

2.6. Paper-based analytical device (PAD) preparation

10 mg of the developed material (PMA_D-TRP) was dispersed in5 mL of nanopure water and filtrated under vacuum to entrap the PMA_D-TRP in the nitrocellulose membrane pores (porosity:

 doi:10.20944/preprints202306.1250.v1

0.45 µm). After filtration, the paper was dried in the oven for 15 min at 40 °C. The paper was then cut into small disks for further use and named as PAD_PMA_D-TRP.

2.7. Adsorption study

10 mg of MMIC/MNIC was introduced into 1 mL of D-TRP with concentration range of 30-320 µM. The mixtures were shaken at a room temperature for 15 min. After the adsorption process, the sorbent was separated by centrifugation at 1000 rpm for 2min. The concentrations of the obtained supernatants were determined by the UV-spectrophotometer at the wavelength of 280 nm. The adsorption capacity (Q_e) was calculated by the following equation (1):

$$\boldsymbol{Q} = \frac{\boldsymbol{C_i - C_e}}{\mathbf{m}} \boldsymbol{V} \qquad (1)$$

2.8. Solid-phase extraction combined with smartphone detection

The solid-phase extraction is a versatile and effective sample preparation technique that enables the selective extraction of target analytes from complex sample matrices. In this work, the proposed MMIC was used as sorbent in solid phase extraction technique for the total TRP isolation. The discrimination between the TRP enantiomers was performed using the developed PAD_PMA_D-TRP. The procedure was as follow: 10 mg of MMIC was introduced into an Eppendorf tube containing 1 mL of TRP solution. The blend was shacked for 30 min at room temperature. After adsorption, the TRP was eluted by 1 mL of methanol and measured with UV spectroscopy at λ = 280 nm to determine the total concentration of L/D-TRP. Then, 10 µL of the supernatant was added to the developed PAD_PMA_D-TRP containing 40 µL of AuNPs dispersion and followed by the addition of 10 µL of Britton-Robinson (BR) buffer (0.04 M H_3PO_4, 0.04 M AcH, 0.04 M H_3BO_3) (pH4). After 25 min, the spots were measured by the smartphone (Scheme 1).

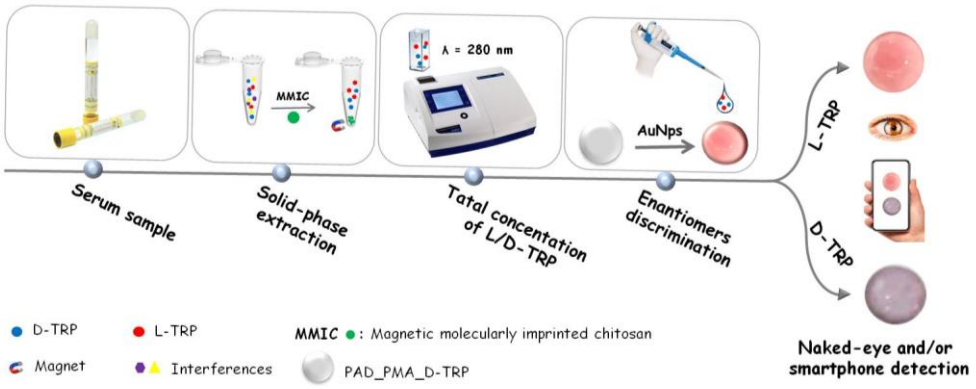

Scheme 1. Illustration of solid-phase extraction coupled with a smartphone discrimination of L/D-TRP enantiomers.

3. Results and discusions

3.1. Characterization studies of Fe_3O_4 and MMIC

FTIR technique was used to analyze the chemical composition and functional groups of the proposed materials **(Fig 1A)**. The Fe_3O_4 typically exhibited the absorption bands of O-H stretching vibration at 3200-3600 cm^{-1} (adsorbed water) and a strong band around 550-650cm^{-1} corresponding to Fe-O group. However, the MMIC material presents both characteristic chitosan absorption bands including: O-H at 3200-3600 cm^{-1}, C=O 1650 cm^{-1}, N-H around 1560 $cm^{-1}$and the characteristic bands of Fe_3O_4 mentioned above. These results confirmed the Fe_3O_4 modification with chitosan.

Preprints (www.preprints.org) | NOT PEER-REVIEWED | Posted: 16 June 2023 doi:10.20944/preprints202306.1250.v1

The XRD technique was also performed to confirm the materials preparation **(Fig 1B).**Fe_3O_4 exhibits a characteristic spinel crystal structure, with peaks typically observed at 2θ values around 30°, 35°, 43°, 57°, and 62°, corresponding to the (220), (311), (400), (511), and (440) crystal planes, respectively. The quoted peaks corresponded well with the standard XRD data of magnetic Fe_3O_4 (JCPDS No. 85-1436) [33]. When chitosan is decorated onto Fe_3O_4, the XRD pattern showed changes in the peak intensities. These changes would depend on the interaction between chitosan and Fe_3O_4.

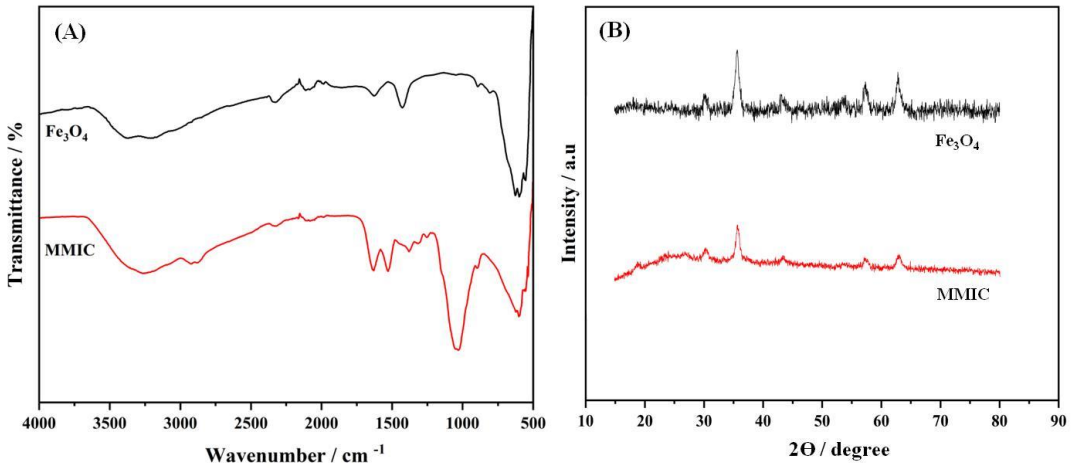

Figure 1. FTIR spectra (A) and XRD diffractograms (B) of Fe_3O_4 and MMIC, respectively.

3.2. Scanning/transmission electron microscopy

STEM images were acquired to assess the behavior of AuNPs when exposed to D-TRP or L-TRP. As depicted in **Fig 2A** and **2B**, the presence of D-TRP led to the aggregation of AuNPs, causing them to cluster together. Conversely, in the presence of L-TRP, the AuNPs remained dispersed and exhibited a monodisperse distribution.

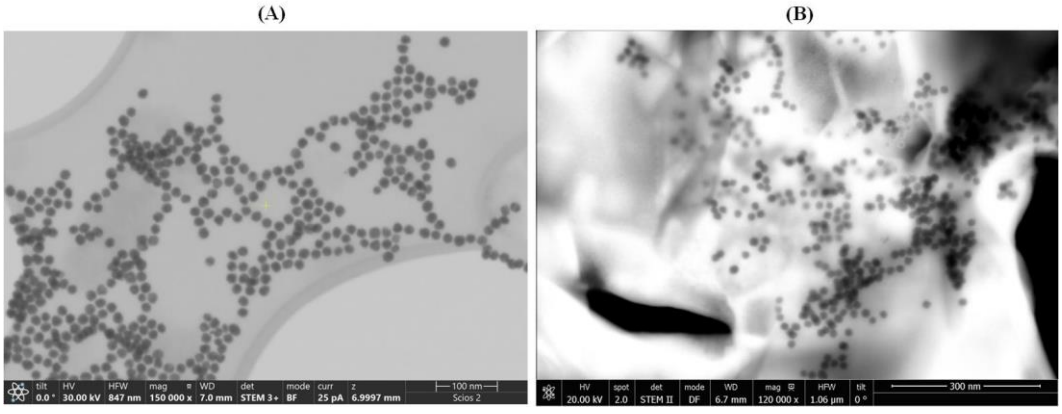

Figure 2. STEM images of AuNPs/L-TRP (A), and AuNPs/D-TRP(B). Micrographs were taken at different magnifications (×150,000 and ×120,000) and in bright (BF) and dark (DF) field modes, respectively.

3.3. Adsorption study

The adsorption study plays a crucial role in the characterization of MIPs by providing insights into binding capacity. It contributes to the understanding of MIP behavior and aid in the developemt of efficient and highly specific cavities to the analyte.

The binding isotherms of D-TRP on the MMIC and MNIC at 25 °C are presented in **Fig 3**. As the concentration of D-TRP increased, both the MMIC and MNIC demonstrated higher binding capaci-

 doi:10.20944/preprints202306.1250.v1

ties. However, due to the presence of multiple cavities, the MMIC exhibited a higher adsorption capacity compared to the MNIC. This observation was supported by the higher values of the imprinted factor, which represents the ratio of the adsorption capacity of MMIC to MNIC. The imprinted factor values ranged between 1.5 and 2, providing further evidence for the successful development of D-TRP cavities on the surface of the MMIC.

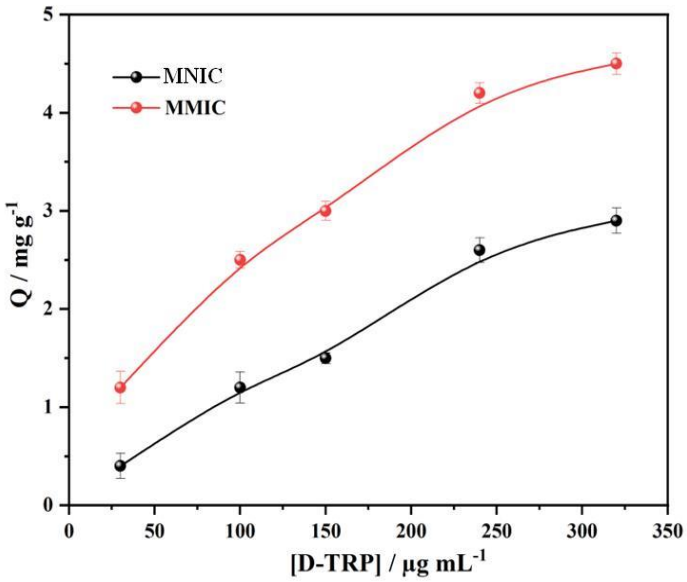

Figure 3. Adsorption isotherms of D-TRP on MMIC and MNIC at room temperature.

3.4. Discrimination between TRP enantiomers

Discrimination between the two enantiomers of tryptophan is important for several reasons including protein synthesis, neurotransmitter production, drug development, and understanding metabolism and health. In the present work, the discrimination was performed after the extraction of total TRP using the developed MMIC. Indeed, a paper-based analytical device was developed for the discrimination between the TRP enantiomers**.** This device is based on a membrane modified with polymethacrylic acid grafted with D-TRP (PAD_PMA_D-TRP). For the visual detection, the AuNPs were used as colorimetric probe because of their sensitive aggregation with TRP. Indeed, the AuNPs change the coloration from red to purple color by the aggregation phenomenon provided by TRP. The developed PAD_PMA_D-TRP exhibits a high affinity to D-TRP providing a rapid AuNPs aggregation. However, there is no interaction between PAD_PMA_D-TRP and L-TRP thus the AuNPs maintain thier red coloration. This approach enables the convenient discrimination of TRP enantiomers using a smartphone or even with the naked eye.

3.5. Smartphone detection

To enable on-site quantitative application of the color change exhibited by AuNPs in the presence of TRP, we combined our PAD_PMA_D-TRP with a smartphone. This allowed us to monitor the alterations in RGB values as the red color of AuNPs transitioned to a purplish-blue upon the addition of TRP. The standard RGB scale employs whole-number values ranging from 0 to 255 to represent the intensity of each color channel: red, green, and blue. In this scale, [255,255,255] corresponds to pure white, while [0,0,0] represents absolute black [34–36]. By utilizing Smartphone-based RGB detection, we were able to observe and record the changes in color. The RGB values were measured by image J software, and the difference between red and blue (R-B) values was plotted against the TRP concentration.

Preprints (www.preprints.org) | NOT PEER-REVIEWED | Posted: 16 June 2023 doi:10.20944/preprints202306.1250.v1

3.6. Optimization of the detection procedure

Volume of AuNPs, pH conditions, and time of color developement are the most important parameters to be optimized in order to achieve an effective discrimination between TRP enantiomers.

As mentioned before, the AuNPs were used as colorimetric probe for the TRP discrimination. Thus, the volume of AuNPs is a relevant parameter to be optimized. **Fig 4A.** Showed that 40 µL of AuNPs was the suitable volume to be added onto the PAD_PMA_D-TRP for the colorimetric discrimination between of L-TRP and D-TRP enantiomers.

The aggregation of AuNPs depends on the pH solution (**Fig 4B**.). Indeed, the pH effect of BR buffer was studied in the range of 4 - 11.5. The good interaction between D-TRP and AuNPs was obtained at the pH values of 4. However, the L-TRP has no effect on the AuNPs coloration. Furthermore, the time effect on the discrimination between the TRP enantiomers was also performed (**Fig 4C**). The addition of D-TRP showed significant decrease of R-B intensity compared with L-TRP. A significant deference between L-TRP and D-TRP was obtained at 25 min. Therefore, this time value was utilized for subsequent experiments.

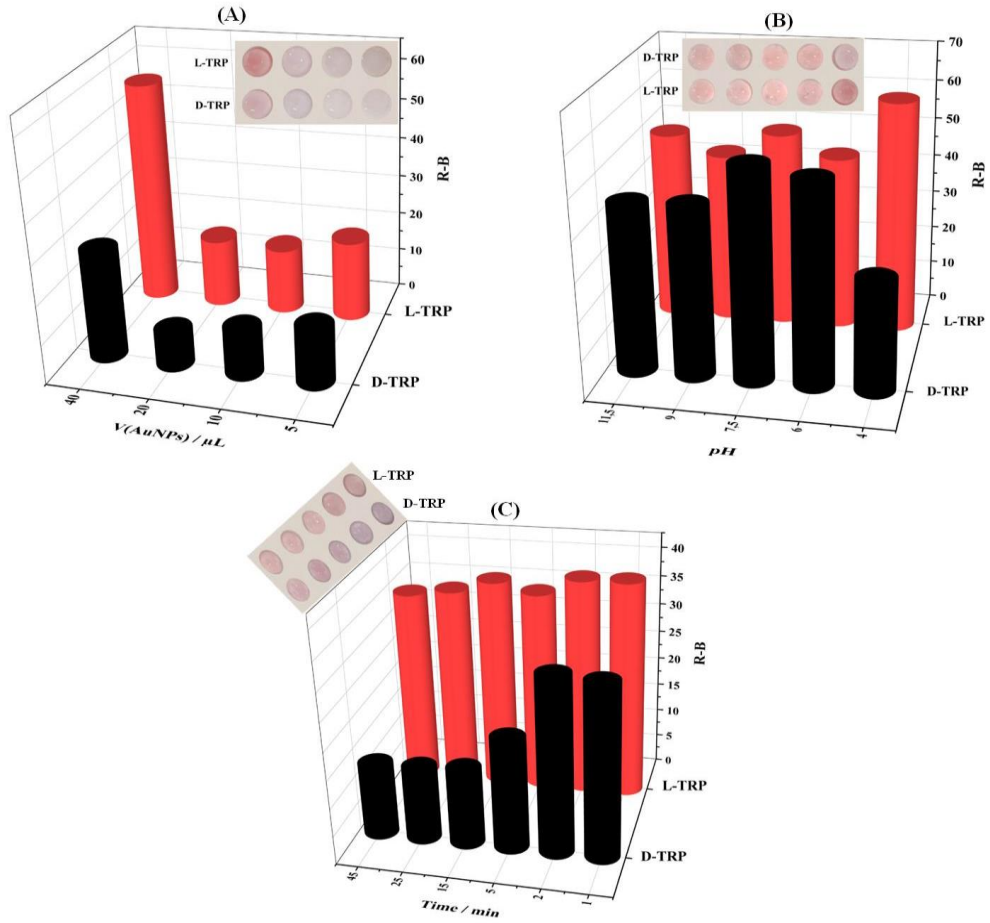

Figure 4. Effect of different parameters on the optimal TRP enantiomers discrimination including: (A) AuNPs volume (pH4 and t = 25 min), (B) optimal pH (V(AuNPs)=40µL and t = 25 min), and (C) time of the color development (V(AuNPs)=40 µL, pH4).

3.7. Calibration curve

Figure 5. A. shows the calibration curves of D-TRP and L-TRP obtained using different concentrations ranging from 10 to 300 µM. As shown in the photographs, the PAD_PMA_D-TRP color changed from the pink to the purple color and becomes more intense with increasing the concentration of D-TRP; thus, the aggregation of the AuNPs occurred. However, by the addition of L-TRP the

Preprints (www.preprints.org) | NOT PEER-REVIEWED | Posted: 16 June 2023 doi:10.20944/preprints202306.1250.v1

PAD_PMA_D-TRP showed no significant color change, indicating the low interaction between L-TRP and the developed material. To quantitatively evaluate the results, the color density is converted into the R-B color intensity. This relationship can be described by the equation: R-B = -0.15 X + 57, where X represents the concentration of the analyte. The correlation coefficient for this linear relationship is 0.986, indicating a strong association. The limit of detection (LOD) for D-TRP was determined to be 3.3 µM, whereas the LOD for L-TRP could not be calculated due to the absence of a significant color change. These findings are based on three individual assays (n=3).

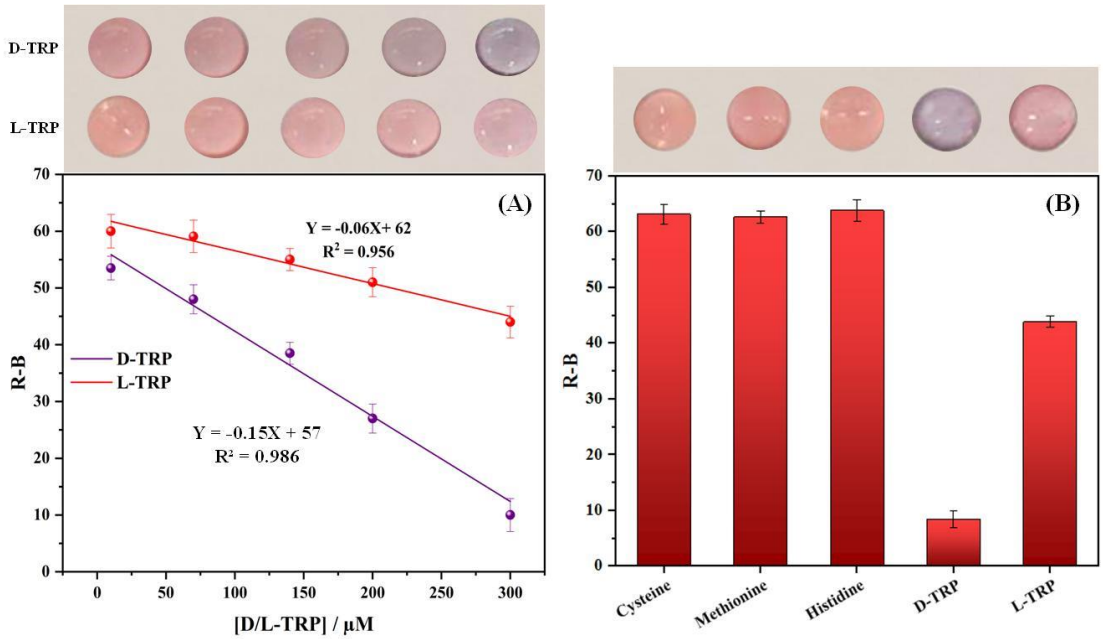

Fig5. The change in color intensity (R-B) as a function of *D*- and *L*-TRP concentration between 10 and 300µM for the optimized assay (A).Selectivity study of the developed device: PAD_PMA_D-TRP (B).

3.8. Selectivity study

The selectivity study plays a pivotal role in ensuring accurate and reliable analysis by identifying target analytes and eliminating interferences. The response of the devoloped PAD_PMA_D-TRP was tested with other amino acids, including cysteine, methionine, histidine, and L-TRP. **Fig 5B** presents the results obtained under the optimal conditions. It is evident that only D-TRP exhibited a lower R-B response compared to the other amino acids. Notably, L-cysteine was found to cause aggregation of the AuNPs. However, the use of the MMIC in sample preparation effectively removed interferents like L-cysteine thank to its specific cavities, which are complementary only to TRP in terms of shape, size and functional groups. By combining the MMIC with the developed PAD_PMA_D-TRP, a successful discrimination of TRP enantiomers was achieved.

3.9. Enantioselective measurement of L/D tryptophan mixtures

The primary objective was to investigate whether the discriminative sensing capability of AuNPs could be utilized for determining the enantiomeric percentage using PAD_PMA_D-TRP. Since TRP commonly exists as enantiomeric pairs, it is crucial to assess the influence of one enantiomer on the other. With the proposed approach, we were able to directly evaluate the performance of PAD_PMA_D-TRP in determining the percentage and confirming the enantioselective separation and purification of TRP in a racemic solution using AuNPs. Indeed, after the preparation of the samples using the developed MMIC, the concentration of L/D-TRP in the resulting supernatant can be determined by measuring the total concentration at280 nm using UV spectroscopy. Subsequently, the percentage of each enantiomer can be determined using PAD_PMA_D-TRP.

Preprints (www.preprints.org) | NOT PEER-REVIEWED | Posted: 16 June 2023 doi:10.20944/preprints202306.1250.v1

An interesting observation is related to the color change from red to purple, which is dependent on the enantiomeric ratio. **Fig 6.** illustrates that the aggregation of AuNPs is selectively induced by D-TRP, leading to the precipitation of D-TRP with AuNPs. As a result, an excess of the other enantiomer remains in the solution, thereby enabling enantioseparation. The graph in **Fig 6** demonstrates a linear decrease in R-B intensity with increasing enantiomeric percentage of D-TRP, ranging from 0% to 100%, indicating the optimized assay ability to quantify the enantiomeric composition accurately.

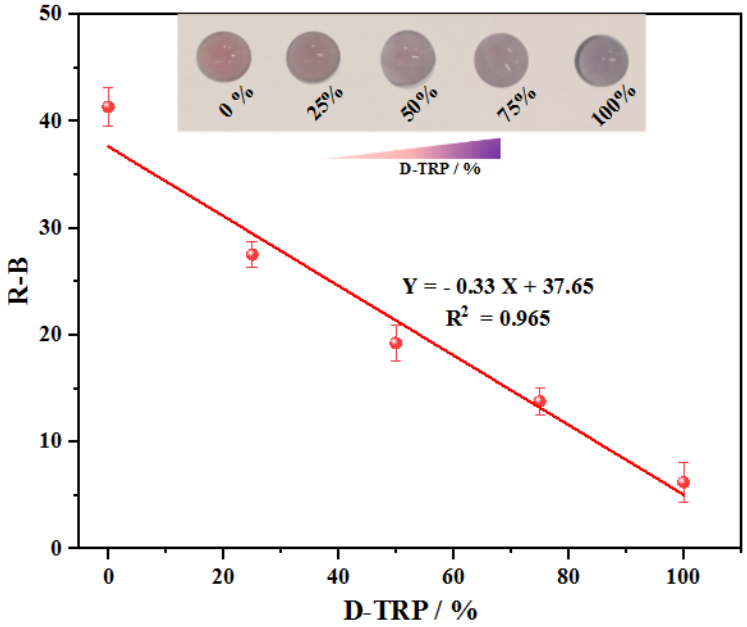

Figure 6. The linear decrease of R-B response as a function of D-TRP (%) in the range from 0% to 100%. Total concentration of L/D-TRP is 300 μM.

3.11. Real sample

Aiming at performing the proposed PAD_PMA_D-TRP for a biological sample, it was utilized for the determination of D-TRP in a human serum sample. The samples spiked with30 and 100 μM of D-TRP were tested. The results are presented in **Table 1** along with satisfactory recoveries between of 88.6–106.4%. The obtained results confirmed the applicability of the developed device for the detection of D-TRP in real biological samples.

Table 1. The application of the proposed method for the determination of D-TRP in a spiked human serum sample.

Added (μM)	Found (μM)	Recovery (%)	RSD (%)*
30	26.5	88.6	3.4
100	106.4	106.4	2.7

*n = 3

 doi:10.20944/preprints202306.1250.v1

4. Conclusions

The discrimination of the enantiomers is necessary in order to understand their distinct biological activities, ensure the safety and efficacy of chiral drugs, and achieve analytical accuracy. This study presents a straightforward approach for the chiral selective sensing of TRP enantiomers using AuNPs as colorimetric probe. The combination of MMIC with the developed PAD_PMA_D-TRP enables the chiral recognition of TRP. The detection of TRP enantiomers can be easily read with the naked eye and/or a smartphone. Remarkably, the proposed sensor demonstrates the capability to detect D-TRP in human serum, suggesting its potential as a valuable platform for analyzing real samples. This paper-based device represents the first example of a simple, cost-effective, and user-friendly platform for enantioselective sensing applications. The success of this application opens up new possibilities for designing innovative enantiosensing strategies in the future.

Author Contributions: Abdelhafid Karrat: Conceptualization, Methodology, Investigation, Visualization, Formal analysis, Writing – original draft**. Juan José García-Guzmán:** Validation, Project administration, writing – reviewing and editing. **José María Palacios-Santander:** Supervision, Conceptualization, Funding acquisition, Project administration, Writing – review & editing. **Aziz Amine:** Supervision, Conceptualization, Project administration, Writing – review & editing. **Laura Cubillana-Aguilera:** Funding acquisition, Resources, Writing – review & editing, Visualization.

Acknowledgments: Abdelhafid Karrat gratefully acknowledges financial support from Erasmus+ KA107 (EU) Program of the University of Cádiz (Spain),through 'Servicio Español para la Internacionalización de la Educación'(SEPIE). Spanish authors thank Agencia Estatal de Investigación (AEI), Ministerio de Ciencia e Innovación of Spain and FEDER funds (EU) for the 'Multibioanalysis' research project (Proyecto de Generación del Conocimiento, PID2021-122578NB-I00) financed by MCIN/AEI/10.13039/501100011033/FEDER, UE"ERDF A way of making Europe". They also thank 'Plan Propio 2022–2023' from University of Cadiz for their funding through the "Acceso al uso de Servicios Centrales de Investigación. Financiación de Actividades"(Ref: SC2022–001)and the "Proyectos Noveles" para impulsar su Carrera Científica"(Ref: PR2022-025, SENSPOT) programs. Authors thank the TEP-243 research group for the support regarding the ATR-FTIR spectra. Finally, the authors also acknowledge Electron Microscopy and X-Ray Diffraction and Fluorescence Divisions from Servicios Centrales de Investigación Científica y Tecnológica of University of Cadiz (SC-ICYT-UCA) for their technical assistance during STEM and XRD measurements.

Conflicts of Interest: The authors declare no conflict of interest

References

1. Fanali, C. Enantiomers Separation by Capillary Electrochromatography. *TrAC - Trends in Analytical Chemistry* **2019**, *120*, 115640, doi:10.1016/j.trac.2019.115640.
2. Makowski, K.; Mera, P.; Paredes, D.; Herrero, L.; Ariza, X.; Asins, G.; Hegardt, F.G.; García, J.; Serra, D. Differential Pharmacologic Properties of the Two C75 Enantiomers: (+)-C75 Is a Strong Anorectic Drug; (−)-C75 Has Antitumor Activity: STEREOSELECTIVITY OF C75 ENANTIOMERS. *Chirality* **2013**, *25*, 281–287, doi:10.1002/chir.22139.
3. Mori, T.; Ito, T.; Liu, S.; Ando, H.; Sakamoto, S.; Yamaguchi, Y.; Tokunaga, E.; Shibata, N.; Handa, H.; Hakoshima, T. Structural Basis of Thalidomide Enantiomer Binding to Cereblon. *Scientific Reports* **2018**, *8*, 1–14, doi:10.1038/s41598-018-19202-7.
4. Li, H.; Wang, L.; Yan, S.; Chen, J.; Zhang, M.; Zhao, R.; Niu, X.; Wang, K. Fusiform-like Metal-Organic Framework for Enantioselective Discrimination of Tryptophan Enantiomers. *Electrochimica Acta* **2022**, *419*, 140409, doi:10.1016/j.electacta.2022.140409.
5. Jafari, M.; Tashkhourian, J.; Absalan, G. Chiral Recognition of Tryptophan Enantiomers Using Chitosan-Capped Silver Nanoparticles: Scanometry and Spectrophotometry Approaches. *Talanta* **2018**, *178*, 870–878, doi:10.1016/j.talanta.2017.10.005.
6. Liu, Y.; Li, Z.; Jia, L. Synthesis of Molecularly Imprinted Polymer Modified Magnetic Particles for Chiral Separation of Tryptophan Enantiomers in Aqueous Medium. *Journal of Chromatography A* **2020**, *1622*, doi:10.1016/j.chroma.2020.461147.

7. Le Floc'h, N.; Otten, W.; Merlot, E. Tryptophan Metabolism, from Nutrition to Potential Therapeutic Applications. *Amino Acids* **2011**, *41*, 1195–1205, doi:10.1007/s00726-010-0752-7.
8. Platten, M.; Nollen, E.A.A.; Röhrig, U.F.; Fallarino, F.; Opitz, C.A. Tryptophan Metabolism as a Common Therapeutic Target in Cancer, Neurodegeneration and Beyond. *Nat Rev Drug Discov* **2019**, *18*, 379–401, doi:10.1038/s41573-019-0016-5.
9. Maier, N.M.; Lindner, W. Chiral Recognition Applications of Molecularly Imprinted Polymers: A Critical Review. *Anal Bioanal Chem* **2007**, *389*, 377–397, doi:10.1007/s00216-007-1427-4.
10. Karrat, A.; García-Guzmán, J.J.; Palacios-Santander, J.M.; Amine, A.; Cubillana-Aguilera, L. New Strategies for the Removal of Template from the Ion and Molecularly Imprinted Polymers: Application to the Fast and on-Site Cr(VI) Detection with a Smartphone. *Sensors and Actuators B: Chemical* **2023**, *386*, 133751, doi:10.1016/j.snb.2023.133751.
11. Díaz-Álvarez, M.; Martín-Esteban, A. Molecularly Imprinted Polymer-Quantum Dot Materials in Optical Sensors: An Overview of Their Synthesis and Applications. *Biosensors* **2021**, *11*, 79, doi:10.3390/bios11030079.
12. Rutkowska, M.; Płotka-Wasylka, J.; Morrison, C.; Wieczorek, P.P.; Namieśnik, J.; Marć, M. Application of Molecularly Imprinted Polymers in Analytical Chiral Separations and Analysis. *TrAC Trends in Analytical Chemistry* **2018**, *102*, 91–102, doi:10.1016/j.trac.2018.01.011.
13. El Hani, O.; Karrat, A.; Digua, K.; Amine, A. Advanced Molecularly Imprinted Polymer-Based Paper Analytical Device for Selective and Sensitive Detection of Bisphenol-A in Water Samples. *Microchemical Journal* **2023**, *184*, 108157, doi:10.1016/j.microc.2022.108157.
14. Villa, C.C.; Sánchez, L.T.; Valencia, G.A.; Ahmed, S.; Gutiérrez, T.J. Molecularly Imprinted Polymers for Food Applications: A Review. *Trends in Food Science & Technology* **2021**, *111*, 642–669, doi:10.1016/j.tifs.2021.03.003.
15. Li, R.; Feng, Y.; Pan, G.; Liu, L. Advances in Molecularly Imprinting Technology for Bioanalytical Applications. *Sensors* **2019**, *19*, 177, doi:10.3390/s19010177.
16. Kadhem, A.J.; Gentile, G.J.; Fidalgo de Cortalezzi, M.M. Molecularly Imprinted Polymers (MIPs) in Sensors for Environmental and Biomedical Applications: A Review. *Molecules* **2021**, *26*, 6233, doi:10.3390/molecules26206233.
17. Madikizela, L.M.; Tavengwa, N.T.; Tutu, H.; Chimuka, L. Green Aspects in Molecular Imprinting Technology: From Design to Environmental Applications. *Trends in Environmental Analytical Chemistry* **2018**, *17*, 14–22, doi:10.1016/j.teac.2018.01.001.
18. Ekmen, E.; Bilici, M.; Turan, E.; Tamer, U.; Zengin, A. Surface Molecularly-Imprinted Magnetic Nanoparticles Coupled with SERS Sensing Platform for Selective Detection of Malachite Green. *Sensors and Actuators B: Chemical* **2020**, *325*, 128787, doi:10.1016/j.snb.2020.128787.
19. Moya Betancourt, S.N.; Cámara, C.I.; Riva, J.S. Interaction between Pharmaceutical Drugs and Polymer-Coated Fe3O4 Magnetic Nanoparticles with Langmuir Monolayers as Cellular Membrane Models. *Pharmaceutics* **2023**, *15*, 311, doi:10.3390/pharmaceutics15020311.
20. Chen, Q.; Liu, X.; Yang, H.; Zhang, S.; Song, H.; Zhu, X. Preparation and Evaluation of Magnetic Graphene Oxide Molecularly Imprinted Polymers (MIPs-GO-Fe3O4@SiO2) for the Analysis and Separation of Tripterine. *Reactive and Functional Polymers* **2021**, *169*, 105055, doi:10.1016/j.reactfunctpolym.2021.105055.
21. Poma, A.; Guerreiro, A.; Whitcombe, M.J.; Piletska, E.V.; Turner, A.P.F.; Piletsky, S.A. Solid-Phase Synthesis of Molecularly Imprinted Polymer Nanoparticles with a Reusable Template–"Plastic Antibodies." *Adv Funct Materials* **2013**, *23*, 2821–2827, doi:10.1002/adfm.201202397.
22. Krupadam, R.J.; Patel, G.P.; Balasubramanian, R. Removal of Cyanotoxins from Surface Water Resources Using Reusable Molecularly Imprinted Polymer Adsorbents. *Environ Sci Pollut Res* **2012**, *19*, 1841–1851, doi:10.1007/s11356-011-0703-1.
23. Zouaoui, F.; Bourouina-Bacha, S.; Bourouina, M.; Jaffrezic-Renault, N.; Zine, N.; Errachid, A. Electrochemical Sensors Based on Molecularly Imprinted Chitosan: A Review. *TrAC - Trends in Analytical Chemistry* **2020**, *130*, 115982, doi:10.1016/j.trac.2020.115982.

24. Mulyasuryani, A.; Prananto, Y.P.; Fardiyah, Q.; Widwiastuti, H.; Darjito, D. Application of Chitosan-Based Molecularly Imprinted Polymer in Development of Electrochemical Sensor for p-Aminophenol Determination. *Polymers* **2023**, *15*, 1818, doi:10.3390/polym15081818.
25. Kharroubi, M.; Bellali, F.; Karrat, A.; Bouchdoug, M.; Jaouad, A.; Laboratory of Biotechnologies, Specialized Center of Valorization and Technology of Sea Products, National Institute of Fisheries Research (INRH), Agadir, Morocco; Laboratory of Biological Engineering, Faculty of Science and Technology, Beni Mellal University Sultan Moulay Slimane, Morocco; Research Team of Innovation and Sustainable Development & Expertise in Green Chemistry, "ERIDDECV", Department of Chemistry, Cadi Ayyad University, Marrakesh, Morocco Preparation of *Teucrium Polium* Extract-Loaded Chitosan-Sodium Lauryl Sulfate Beads and Chitosan-Alginate Films for Wound Dressing Application. *AIMSPH* **2021**, *8*, 754–775, doi:10.3934/publichealth.2021059.
26. He, S.; Liu, D.; Wang, Z.; Cai, K.; Jiang, X. Utilization of Unmodified Gold Nanoparticles in Colorimetric Detection. *Sci. China Phys. Mech. Astron.* **2011**, *54*, 1757–1765, doi:10.1007/s11433-011-4486-7.
27. Chang, C.-C.; Chen, C.-P.; Wu, T.-H.; Yang, C.-H.; Lin, C.-W.; Chen, C.-Y. Gold Nanoparticle-Based Colorimetric Strategies for Chemical and Biological Sensing Applications. *Nanomaterials* **2019**, *9*, 861, doi:10.3390/nano9060861.
28. Noviana, E.; Ozer, T.; Carrell, C.S.; Link, J.S.; McMahon, C.; Jang, I.; Henry, C.S. Microfluidic Paper-Based Analytical Devices: From Design to Applications. *Chem. Rev.* **2021**, *121*, 11835–11885, doi:10.1021/acs.chemrev.0c01335.
29. Martinez, A.W.; Phillips, S.T.; Whitesides, G.M.; Carrilho, E. Diagnostics for the Developing World: Microfluidic Paper-Based Analytical Devices. *Anal. Chem.* **2010**, *82*, 3–10, doi:10.1021/ac9013989.
30. Fu, L.-M.; Wang, Y.-N. Detection Methods and Applications of Microfluidic Paper-Based Analytical Devices. *TrAC Trends in Analytical Chemistry* **2018**, *107*, 196–211, doi:10.1016/j.trac.2018.08.018.
31. Afzali, M.; Mostafavi, A.; Shamspur, T. A Novel Electrochemical Sensor Based on Magnetic Core@shell Molecularly Imprinted Nanocomposite (Fe3O4@graphene Oxide@MIP) for Sensitive and Selective Determination of Anticancer Drug Capecitabine. *Arabian Journal of Chemistry* **2020**, *13*, 6626–6638, doi:10.1016/j.arabjc.2020.06.018.
32. Cubillana-Aguilera, L.M.; Franco-Romano, M.; Gil, M.L.A.; Naranjo-Rodríguez, I.; Hidalgo-Hidalgo de Cisneros, J.L.; Palacios-Santander, J.M. New, Fast and Green Procedure for the Synthesis of Gold Nanoparticles Based on Sonocatalysis. *Ultrasonics Sonochemistry* **2011**, *18*, 789–794, doi:10.1016/j.ultsonch.2010.10.009.
33. Li, G.; Jiang, Y.; Huang, K.; Ding, P.; Chen, J. Preparation and Properties of Magnetic Fe3O4–Chitosan Nanoparticles. *Journal of Alloys and Compounds* **2008**, *466*, 451–456, doi:10.1016/j.jallcom.2007.11.100.
34. Upadhyay, Y.; Bothra, S.; Kumar, R.; Sahoo, S.K. Smartphone-Assisted Colorimetric Detection of Cr^{3+} Using Vitamin B_6 Cofactor Functionalized Gold Nanoparticles and Its Applications in Real Sample Analyses. *ChemistrySelect* **2018**, *3*, 6892–6896, doi:10.1002/slct.201801289.
35. Karrat, A.; Amine, A. Paper-Based Analytical Device for One-Step Detection of Bisphenol-A Using Functionalized Chitosan. *Chemosensors* **2022**, *10*, 450, doi:10.3390/chemosensors10110450.
36. Rezazadeh, M.; Seidi, S.; Lid, M.; Pedersen-Bjergaard, S.; Yamini, Y. The Modern Role of Smartphones in Analytical Chemistry. *TrAC Trends in Analytical Chemistry* **2019**, *118*, 548–555, doi:10.1016/j.trac.2019.06.019.